Chapter 2
Actuators and Drive Systems

Actuators are one of the key components contained in a robotic system. A robot has many degrees of freedom, each of which is a servoed joint generating desired motion. We begin with basic actuator characteristics and drive amplifiers to understand behavior of servoed joints.

Most of today's robotic systems are powered by electric servomotors. Therefore, we focus on electromechanical actuators.

2.1 DC Motors

Figure 2-1 illustrates the construction of a DC servomotor, consisting of a stator, a rotor, and a commutation mechanism. The stator consists of permanent magnets, creating a magnetic field in the air gap between the rotor and the stator. The rotor has several windings arranged symmetrically around the motor shaft. An electric current applied to the motor is delivered to individual windings through the brush-commutation mechanism, as shown in the figure. As the rotor rotates the polarity of the current flowing to the individual windings is altered. This allows the rotor to rotate continually.

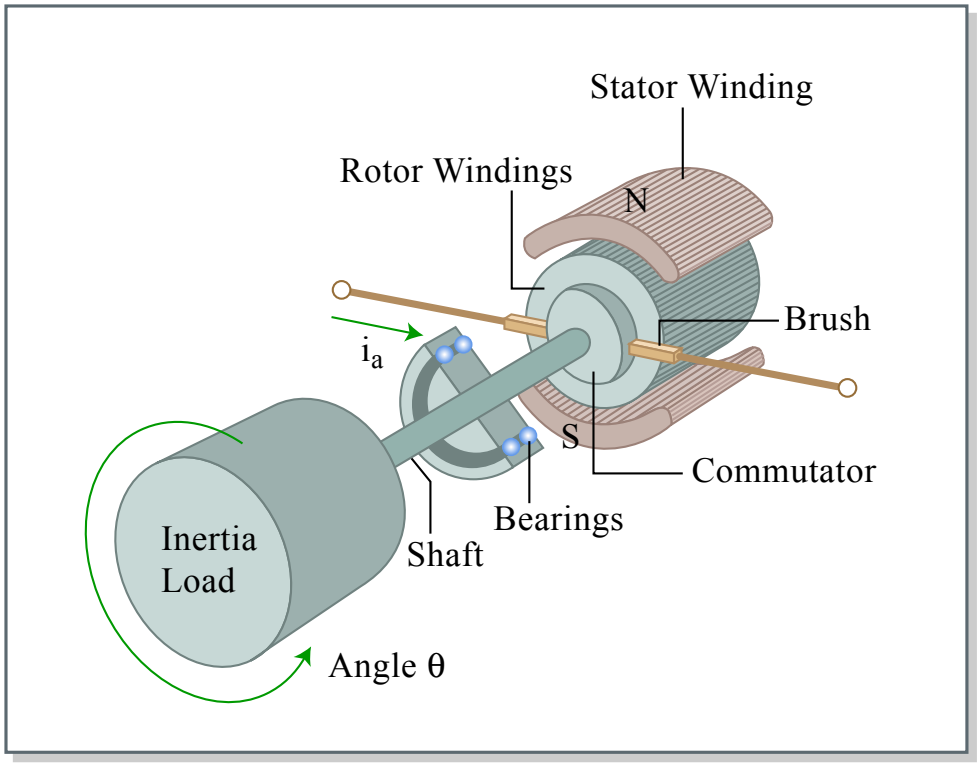

Figure by MIT OCW.

Figure 2.1.1 Construction of DC motor

Let τ_m be the torque created at the air gap, and i the current flowing to the rotor windings. The torque is in general proportional to the current, and is given by

$$\tau_m = K_t \cdot i \tag{2.1.1}$$

where the proportionality constant K_t is called the ***torque constant,*** one of the key parameters describing the characteristics of a DC motor. The torque constant is determined by the strength of the magnetic field, the number of turns of the windings, the effective area of the air gap, the radius of the rotor, and other parameters associated with materials properties.

In an attempt to derive other characteristics of a DC motor, let us first consider an idealized energy transducer having no power loss in converting electric power into mechanical

power. Let E be the voltage applied to the idealized transducer. The electric power is then given by $E \cdot i$, which must be equivalent to the mechanical power:

$$P_{in} = E \cdot i = \tau_m \cdot \omega_m \tag{2.1.2}$$

where ω_m is the angular velocity of the motor rotor. Substituting eq.(1) into eq.(2) and dividing both sides by i yield the second fundamental relationship of a DC motor:

$$E = K_t \omega_m \tag{2.1.3}$$

The above expression dictates that the voltage across the idealized power transducer is proportional to the angular velocity and that the proportionality constant is the same as the torque constant given by eq.(1). This voltage E is called the back emf (electro-motive force) generated at the air gap, and the proportionality constant is often called the back emf constant.

Note that, based on eq.(1), the unit of the torque constant is *Nm/A* in the metric system, whereas the one of the back emf constant is *V/rad/s* based on eq.(2).

Exercise 2.1 Show that the two units, *Nm/A* and *V/rad/s*, are identical.

The actual DC motor is not a loss-less transducer, having resistance at the rotor windings and the commutation mechanism. Furthermore, windings may exhibit some inductance, which stores energy. Figure 2.1.2 shows the schematic of the electric circuit, including the windings resistance R and inductance L. From the figure,

$$u = R \cdot i + L\frac{di}{dt} + E \tag{2.1.4}$$

where u is the voltage applied to the armature of the motor.

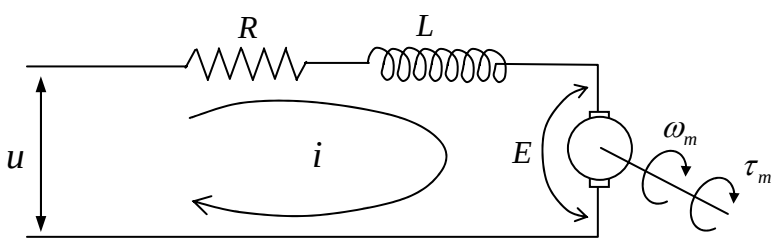

Figure 2.1.2 Electric circuit of armature

Combining eqs.(1), (3) and (4), we can obtain the actual relationship among the applied voltage u, the rotor angular velocity ω_m, and the motor torque τ_m.

$$\frac{K_t}{R}u = \tau_m + T_e\frac{d\tau_m}{dt} + \frac{K_t^{\,2}}{R}\omega_m \tag{2.1.5}$$

where time constant $T_e = \frac{L}{R}$, called the motor reactance, is often negligibly small. Neglecting this second term, the above equation reduces to an algebraic relationship:

$$\tau_m = \frac{K_t}{R} u - \frac{K_t^{\ 2}}{R} \omega_m \tag{2.1.6}$$

This is called the torque-speed characteristic. Note that the motor torque increases in proportion to the applied voltage, but the net torque reduces as the angular velocity increases. Figure 2.1.3 illustrates the torque-speed characteristics. The negative slope of the straight lines, $-K_t^{\ 2}/R$, implies that the voltage-controlled DC motor has an inherent damping in its mechanical behavior.

The power dissipated in the DC motor is given by

$$P_{dis} = R \cdot i^2 = \frac{R}{K_t^{\ 2}} \tau_m^{\ 2} \tag{2.1.7}$$

from eq.(1). Taking the square root of both sides yields

$$\sqrt{P_{dis}} = \frac{\tau_m}{K_m}, \quad K_m = \frac{K_t}{\sqrt{R}} \tag{2.1.8}$$

where the parameter K_m is called the motor constant. The motor constant represents how effectively electric power is converted to torque. The larger the motor constant becomes, the larger the output torque is generated with less power dissipation. A DC motor with more powerful magnets, thicker winding wires, and a larger rotor diameter has a larger motor constant. A motor with a larger motor constant, however, has a larger damping, as the negative slope of the torque-speed characteristics becomes steeper, as illustrated in Figure 2.1.3.

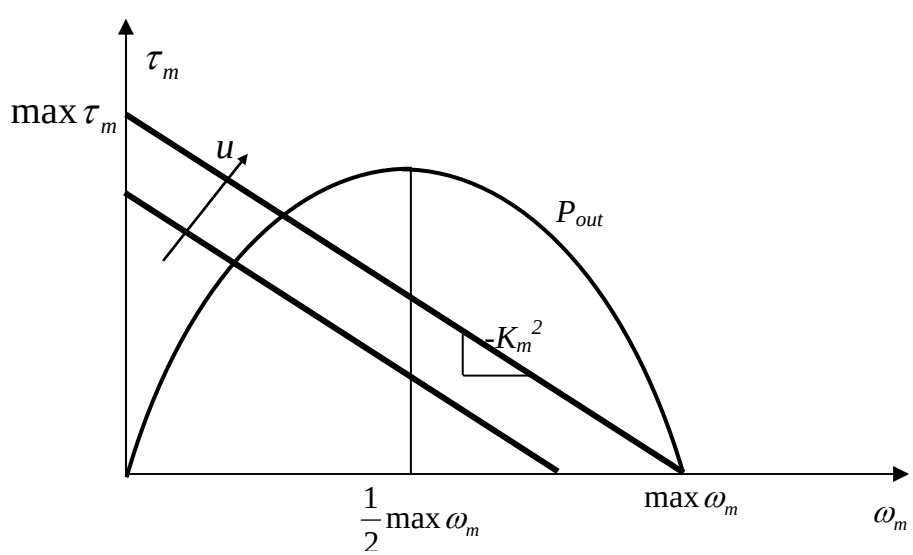

Figure 2.1.3 Torque-speed characteristics and output power

Taking into account the internal power dissipation, the net output power of the DC motor is given by

$$P_{out} = \tau_m \cdot \omega_m = (\frac{K_t}{R} u - K_m{}^2 \omega_m)\, \omega_m \tag{2.1.9}$$

This net output power is a parabolic function of the angular velocity, as illustrated in Figure 2.1.3. It should be noted that the net output power becomes maximum in the middle point of the velocity axis, i.e. 50 % of the maximum angular velocity for a given armature voltage *u*. This implies that the motor is operated most effectively at 50 % of the maximum speed. As the speed departs from this middle point, the net output power decreases, and it vanishes at the zero speed as well as at the maximum speed. Therefore, it is important to select the motor and gearing combination so that the maximum of power transfer be achieved.

2.2 Dynamics of Single-Axis Drive Systems

DC motors and other types of actuators are used to drive individual axes of a robotic system. Figure 2.2.1 shows a schematic diagram of a single-axis drive system consisting of a DC motor, a gear head, and arm links[1]. An electric motor, such as a DC motor, produces a relatively small torque and rotates at a high speed, whereas a robotic joint axis in general rotates slowly, and needs a high torque to bear the load. In other words, the impedance of the actuator:

$$Z_m = \frac{torque}{angular\ velocity} = \frac{\tau_m}{\omega_m} \tag{2.2.1}$$

is much smaller than that of the load.

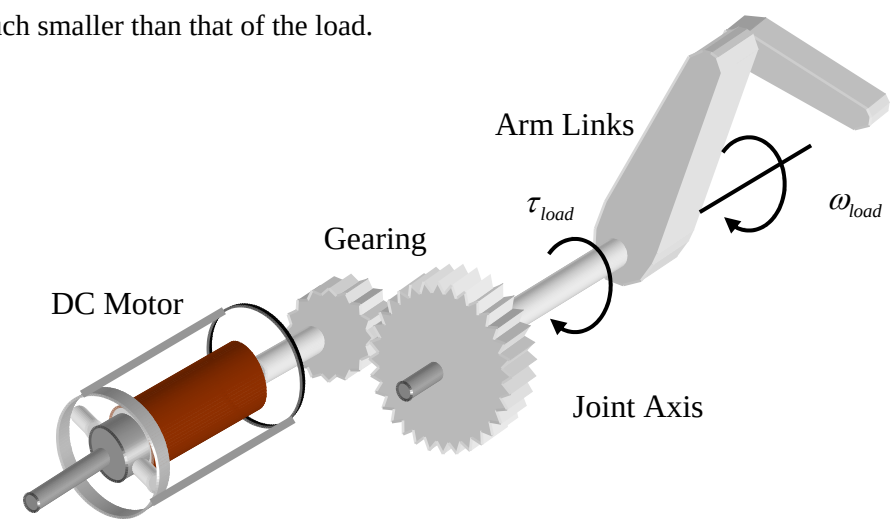

Figure 2.2.1 Joint axis drive system

[1] Although a robotic system has multiple axes driven by multiple actuators having dynamic interactions, we consider behavior of an independent single axis in this section, assuming that all the other axes are fixed.

To fill the gap we need a gear reducer, as shown in Figure 2.2.1. Let $r > 1$ be a gear reduction ratio (If d_1 and d_2 are diameters of the two gears, the gear reduction ratio is $r = d_2 / d_1$). The torque and angular velocity are changed to:

$$\tau_{load} = r \cdot \tau_m, \quad \omega_{load} = \frac{1}{r}\omega_m \tag{2.2.2}$$

where τ_{load} and ω_{load} are the torque and angular velocity at the joint axis, as shown in the figure. Note that the gear reducer of gear ratio r increases the impedance r^2 times larger than that of the motor axis Z_m:

$$Z_{load} = r^2 \cdot Z_m \tag{2.2.3}$$

Let I_m be the inertia of the motor rotor. From the free body diagram of the motor rotor,

$$I_m \dot{\omega}_m = \tau_m - \frac{1}{r}\tau_{load} \tag{2.2.4}$$

where $-\frac{1}{r}\tau_{load}$ is the torque acting on the motor shaft from the joint axis through the gears, and $\dot{\omega}_m$ is the time rate of change of angular velocity, i.e. the angular acceleration. Let I_l be the inertia of the arm link about the joint axis, and b the damping coefficient of the bearings supporting the joint axis. Considering the free body diagram of the arm link and joint axis yields

$$I_l \dot{\omega}_{load} = \tau_{load} - b\omega_{load} \tag{2.2.5}$$

Eliminating τ_{load} from the above two equations and using eq.(2.1.6) and (2.2.2) yields

$$I\dot{\omega}_{load} + B\omega_{load} = k \cdot u \tag{2.2.6}$$

where I, B, k are the effective inertia, damping, and input gain reflected to the joint axis:

$$I = I_l + r^2 I_m \tag{2.2.7}$$

$$B = b + r^2 K_m{}^2 \tag{2.2.8}$$

$$k = r\frac{K_t}{R} \tag{2.2.9}$$

Note that the effective inertia of the motor rotor is r^2 times larger than the original value I_m when reflected to the joint axis. Likewise, the motor constant becomes r^2 times larger when reflected to the joint axis. The gear ratio of a robotic system is typically 20 ~ 100, which means that the effective inertia and damping becomes 400 ~ 10,000 times larger than those of the motor itself.

For fast dynamic response, the inertia of the motor rotor must be small. This is a crucial requirement as the gear ratio gets larger, like robotics applications. There are two ways of

reducing the rotor inertia in motor design. One is to reduce the diameter and make the rotor longer, as shown in Figure 2.2.2-(a). The other is to make the motor rotor very thin, like a pancake, as shown in Figure 2.2.2-(b).

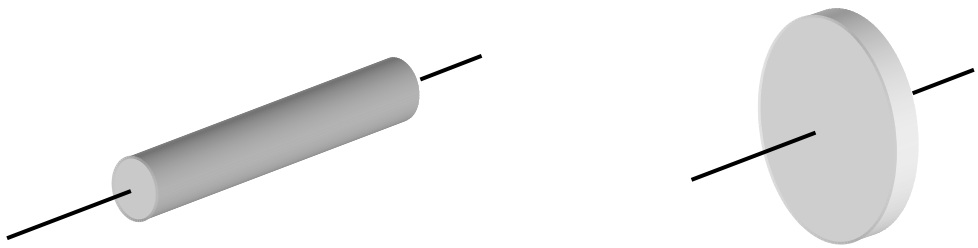

(a) Long and slender (b) Pancake

Figure 2.2.2 Two ways of reducing the motor rotor inertia

Most robots use the long and slender motors as Figure (a), and some heavy-duty robots use the pancake type motor. Figure 2.2.3 shows a pancake motor by Mavilor Motors, Inc.

Figure removed for copyright reasons.

Figure 2.2.3 Pancake DC motor

Exercise 2-2 Assuming that the angular velocity of a joint axis is approximately zero, obtain the optimal gear ratio *r* in eq.(7) that maximizes the acceleration of the joint axis.

2.3 Power Electronics

Performance of servomotors used for robotics applications highly depends on electric power amplifiers and control electronics, broadly termed power electronics. Power electronics has shown rapid progress in the last two decades, as semiconductors became faster, more powerful, and more efficient. In this section we will briefly summarize power electronics relevant to robotic system development.

2.3.1 Pulse width modulation (PWM)

In many robotics applications, actuators must be controlled precisely so that desired motions of arms and legs may be attained. This requires a power amplifier to drive a desired level of voltage (or current indirectly) to the motor armature, as discussed in the previous section. Use of a linear amplifier (like an operational amplifier), however, is power-inefficient and impractical, since it entails a large amount of power loss. Consider a simple circuit consisting of a single transistor for controlling the armature voltage, as shown in Figure 2.3.1. Let V be the supply voltage connected to one end of the motor armature. The other end of the armature is connected to the collector of the transistor. As the base voltage varies the emitter-collector voltage varies, and thereby the voltage drop across the motor armature, denoted u in the figure, varies accordingly. Let i be the collector current flowing through the transistor. Then the power loss that is dissipated at the transistor is given by

$$P_{loss} = (V-u)\cdot i = \frac{1}{R}(V-u)\cdot u \tag{2.3.1}$$

where R is the armature resistance. Figure 2.3.2 plots the internal power loss at the transistor against the armature voltage. The power loss becomes the largest in the middle, where half the supply voltage $V/2$ acts on the armature. This large heat loss is not only wasteful but also harmful, burning the transistor in the worst case scenario. Therefore, this type of linear power amplifier is seldom used except for driving very small motors.

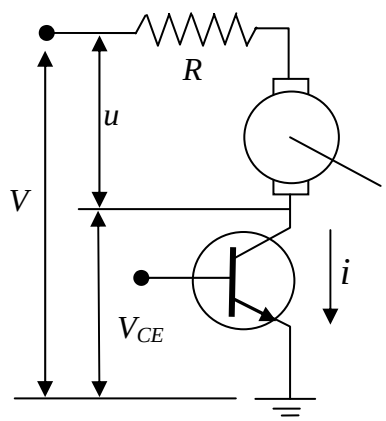

Figure 2.3.1 Analogue power amplifier for driving the armature voltage

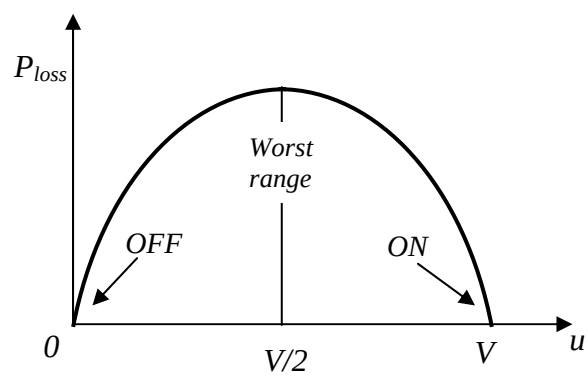

Figure 2.3.2 Power loss at the transistor vs. the armature voltage.

An alternative is to control the voltage via ON-OFF switching. Pulse Width Modulation, or PWM for short, is the most commonly used method for varying the average voltage to the motor. In Figure 2.3.2 it is clear that the heat loss is zero when the armature voltage is either 0 or V. This means that the transistor is completely shutting down the current (OFF) or completely

admitting the current (ON). For all armature voltages other than these complete ON-OFF states, some fraction of power is dissipated in the transistor. Pulse Width Modulation (PWM) is a technique to control an effective armature voltage by using the ON-OFF switching alone. It varies the ratio of time length of the complete ON state to the complete OFF state. Figure 2.3.3 illustrates PWM signals. A single cycle of ON and OFF states is called the PWM period, whereas the percentage of the ON state in a single period is called *duty rate*. The first PWM signal is of 60% duty, and the second one is 25 %. If the supply voltage is *V=10 volts*, the average voltage is *6 volts* and *2.5 volts*, respectively.

The PWM period is set to be much shorter than the time constant associated with the mechanical motion. The PWM frequency, that is the reciprocal to the PWM period, is usually 2 ~ 20 kHz, whereas the bandwidth of a motion control system is at most 100 Hz. Therefore, the discrete switching does not influence the mechanical motion in most cases.

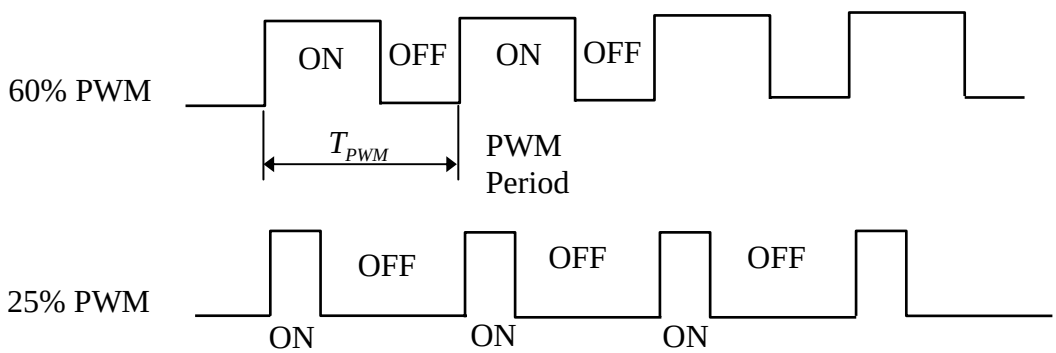

Figure 2.3.3 Pulse width modulation

As modeled in eq.(2.1.4), the actual rotor windings have some inductance L. If the electric time constant T_e is much larger than the PWM period, the actual current flowing to the motor armature is a smooth curve, as illustrated in Figure 2.3.4-(a). In other words, the inductance works as a low-pass filter, filtering out the sharp ON-OFF profile of the input voltage. In contrast, if the electric time constant is too small, compared to the PWM period, the current profile becomes zigzag, following the rectangular voltage profile, as shown in Figure 2.3.4-(b). As a result, unwanted high frequency vibrations are generated at the motor rotor. This happens for some types of pancake motors with low inductance and low rotor inertia.

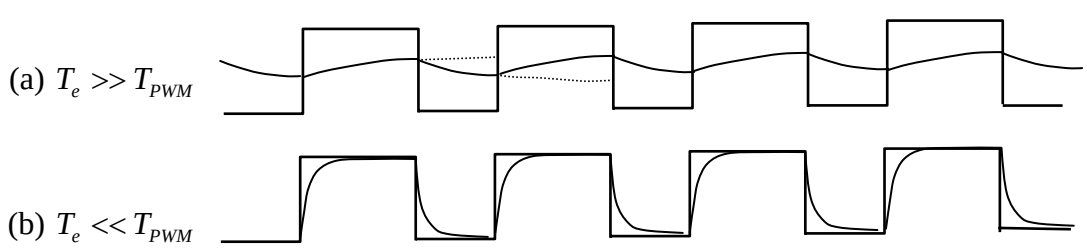

Figure 2.3.4 Current to the motor is smoothed due to inductance

2.3.2 PWM switching characteristics

As the PWM frequency increases, the current driven to the motor becomes smoother, and the nonlinearity due to discrete switching disappears. Furthermore, high PWM frequencies cause no audible noise of switching. The noise disappears as the switching frequency becomes higher

than the human audible range, say *15 kHz*. Therefore, a higher PWM frequency is in general desirable. However, it causes a few adverse effects. As the PWM frequency increases:

- The heat loss increases and the transistor may over-heat,
- Harmful large voltage spikes and noise are generated, and
- Radio frequency interference and electromagnetic interference become prominent.

The first adverse effect is the most critical one, which limits the capacity of a PWM amplifier. Although no power loss occurs at the switching transistor when it is completely ON or OFF, a significant amount of loss is caused during transition. As the transistor state is switched from OFF to ON or vise versa, the transistor in Figure 2.3.1 goes through intermediate states, which entail heat loss, as shown in Figure 2.3.2. Since it takes some finite time for a semiconductor to make a transition, every time it is switched, a certain amount of power is dissipated. As the PWM frequency increases, more power loss and, more importantly, more heat generation occur. Figure 2.3.5 illustrates the turn-on and turn-off transitions of a switching transistor. When turned on, the collector current I_c increases and the voltage V_{ce} decreases. The product of these two values provides the switching power loss as shown by broken lines in the figure. Note that turn-off takes a longer time, hence it causes more heat loss.

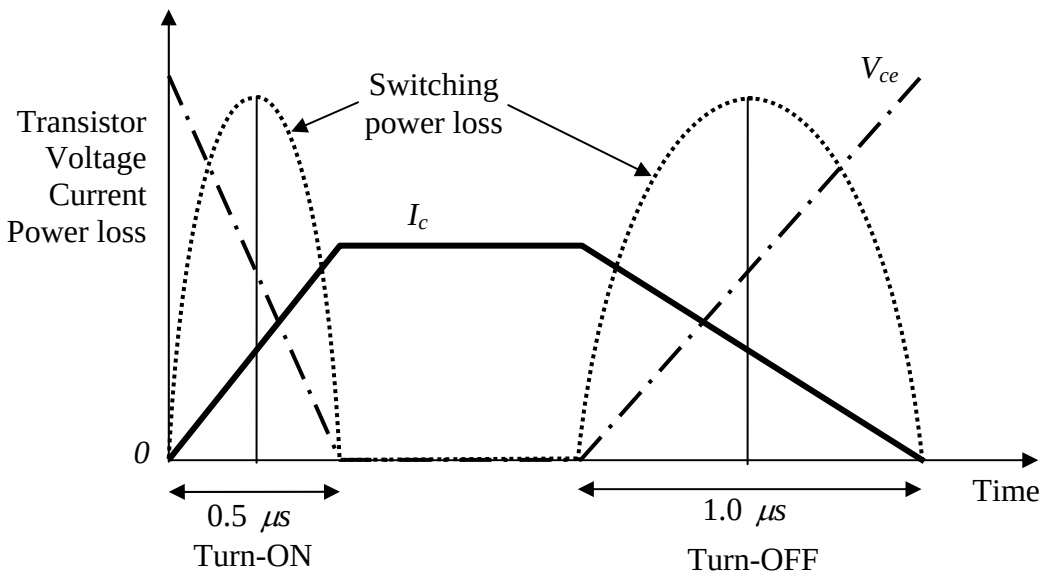

Figure 2.3.5 Transient responses of transistor current and voltage and associated power loss during turn-on and turn-off state transitions

From Figure 2.3.5 it is clear that a switching transistor having fast turn-on and turn-off characteristics is desirable, since it causes less power loss and heat generation. Power MOSFETs (Metal-Oxide-Semiconductor Field-Effect Transistors) have very fast switching characteristics, enabling 15 ~ 100 kHz of switching frequencies. For relatively small motors, MOSFETs are widely used in industry due to their fast switching characteristics. For larger motors, IGBTs (Insulated Gate Bipolar Transistor) are the rational choice because of their larger capacity and relatively fast response.

As the switching speed increases, the heat loss becomes smaller. However, fast switching causes other problems. Consider eq.(2.1.4) again, the dynamic equation of the armature:

$$u = R \cdot i + L\frac{di}{dt} + E \tag{2.1.4}$$

High speed switching means that the time derivative of current *i* is large. This generates a large inductance-induced kickback voltage $L\frac{di}{dt}$ that often damages switching semiconductors. As illustrated in Figure 2.3.6-(a), a large spike is induced when turning on the semiconductor. To get rid of this problem a free-wheeling-diode (FWD) is inserted across the motor armature, as shown in Figure 2.3.6-(b). As the voltage across the armature exceeds a threshold level, FWD kicks in to bypass the current so that the voltage may be clamped, as shown in figure (c).

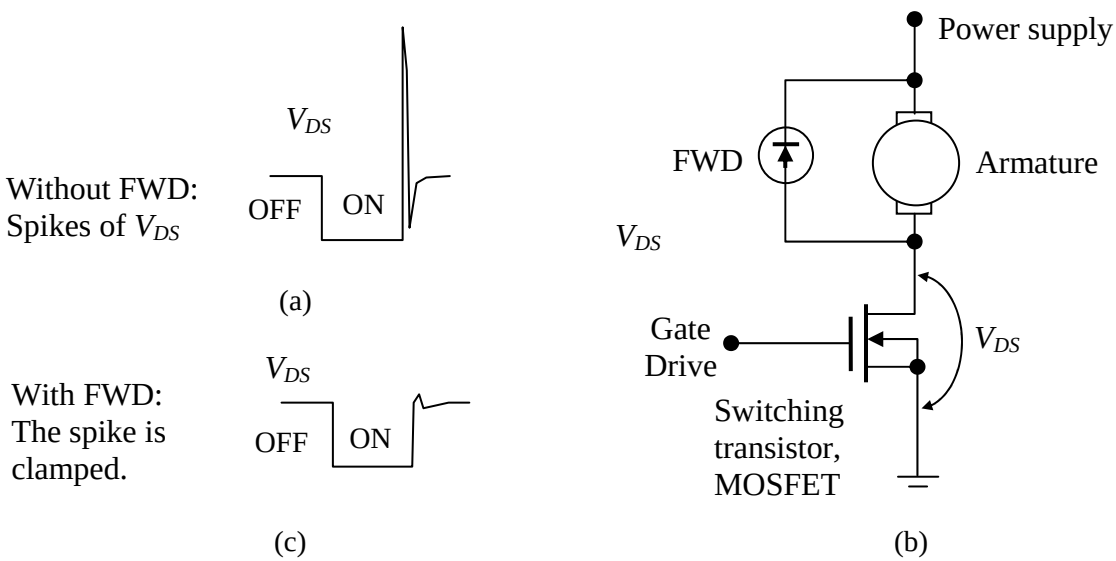

Figure 2.3.6 Voltage spike induced by inductance (a), free-wheeling diode (b), and the clamped spike with FWD (c)

High speed PWM switching also generates Electromagnetic Interference (EMI), particularly when the wires between the PWM amplifier and the motor get longer. Furthermore, high speed PWM switching may incur Radio-Frequency Interference (RFI). Since the PWM waveforms are square, significant RFI can be generated. Whenever PWM switching edges are faster than 10 μs, RFI is induced to some extent. An effective method for reducing EMI and RFI is to put the PWM amplifier inside the motor body. This motor architecture, called Integrated Motor or Smart Motor, allows confining EMI and RFI within the motor body by minimizing the wire length between the motor armature and the power transistors.

2.3.3 The H-bridge and bipolar PWM amplifiers

In most robotics applications, bi-directional control of motor speed is necessary. This requires a PWM amplifier to be bipolar, allowing for both forward and backward rotations. The architecture described in the previous section needs to be extended to meet this bipolar requirement. The H-Bridge architecture is commonly used for bipolar PWM amplifiers. As shown in Figure 2.3.7, the H-Bridge architecture resembles the letter H in the arrangement of switching transistors around the motor armature. Switching transistors A and B are pulled up to the supply voltage *V*, whereas transistors C and D are connected to ground. Combinations of these four switching transistors provide a variety of operations. In figure (i), gates A and D are ON, and B and C are OFF. This gate combination delivers a current to the armature in the

forward direction. When the gate states are reversed, as shown in figure (ii), the direction of current is reversed. Furthermore, the motor coasts off when all the gates are turned OFF, since the armature is totally isolated or disconnected as shown in figure (iii). On the other hand, the armature windings are shortened, when both gates C and D are turned ON and A and B are turned OFF. See figure (iv). This shortened circuit provides a “braking” effect, when the motor rotor is rotating.

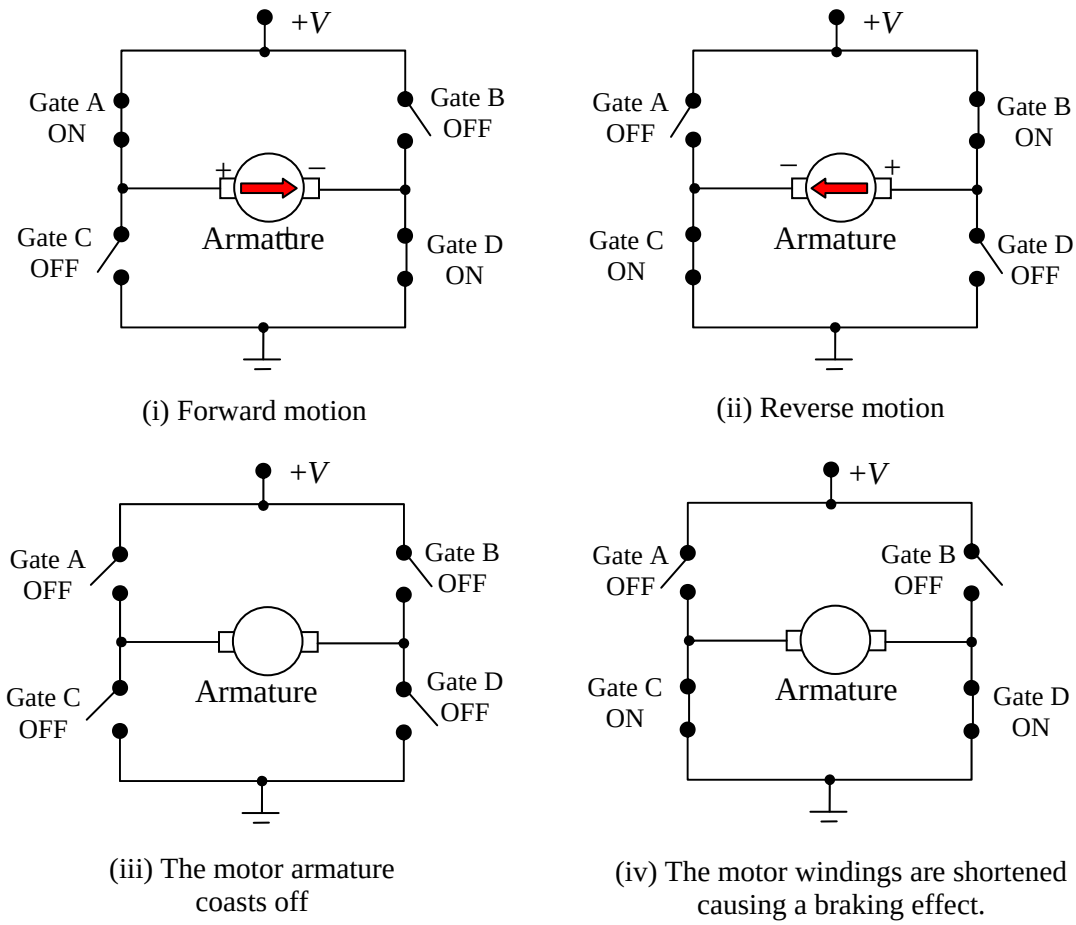

Figure 2.3.7 H-bridge and four quadrant control

It should be noted that there is a fundamental danger in the H-bridge circuit. A direct short circuit can occur if the top and bottom switches connected to the same armature terminal are turned on at the same time. A catastrophic failure results when one of the switching transistors on the same vertical line in Figure 2.3.7 fails to turn off before the other turns on. Most of H-bridge power stages commercially available have several protection mechanisms to prevent the direct short circuit.

2.4 Robot Controls and PWM Amplifiers of the 2.12 Laboratory

DC motors and PWM amplifiers, the two most important components involved in a robot power train, have been described. Now we are ready to introduce the specific drive system and controls to be used for building robots for the design project.

This term we will use controllers and drives produced by Innovation First, Inc. The system consists of bipolar PWM amplifiers, a PIC-based on-board robot controller with a wireless modem, a stationary controller hooked up to a laptop computer. Potentiometers are used for

measuring the angular displacement of joint axes. They are connected to A/D converter ports of the on-board controller for position feedback control. Additional sensors can be hooked up to the on-board controllers. A C-language based development environment is available for the system.

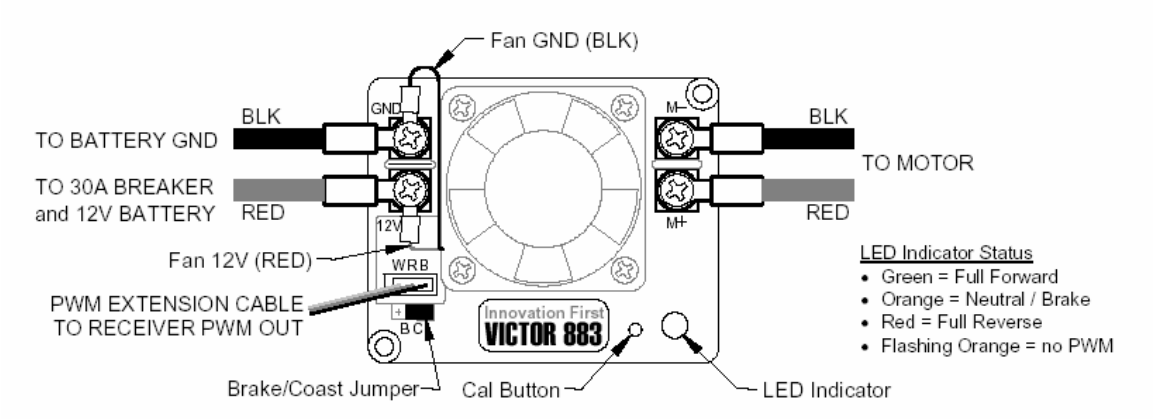

Figure 2.4.1 Bipolar PWM amplifier with a built-in cooling fun, IFI, Inc.

Courtesy of IFI Robotics. Used with permission.

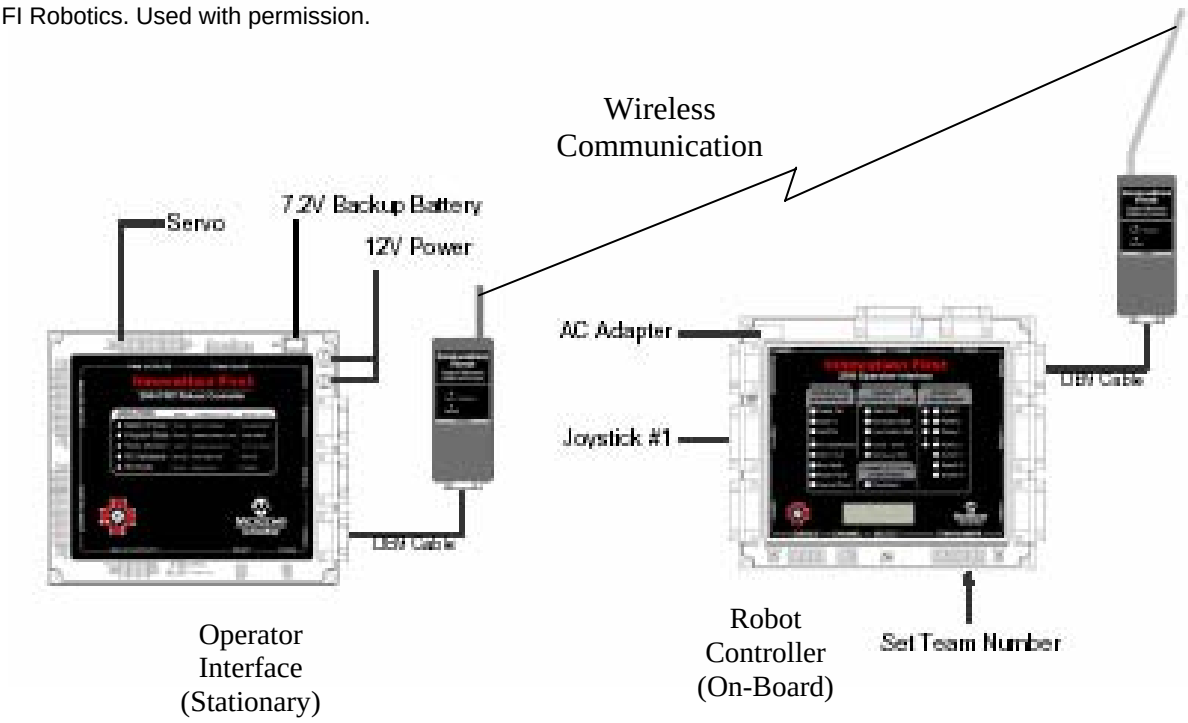

Figure 2.4.2 On-board and stationary controllers, IFI.Inc.

Courtesy of IFI Robotics. Used with permission.

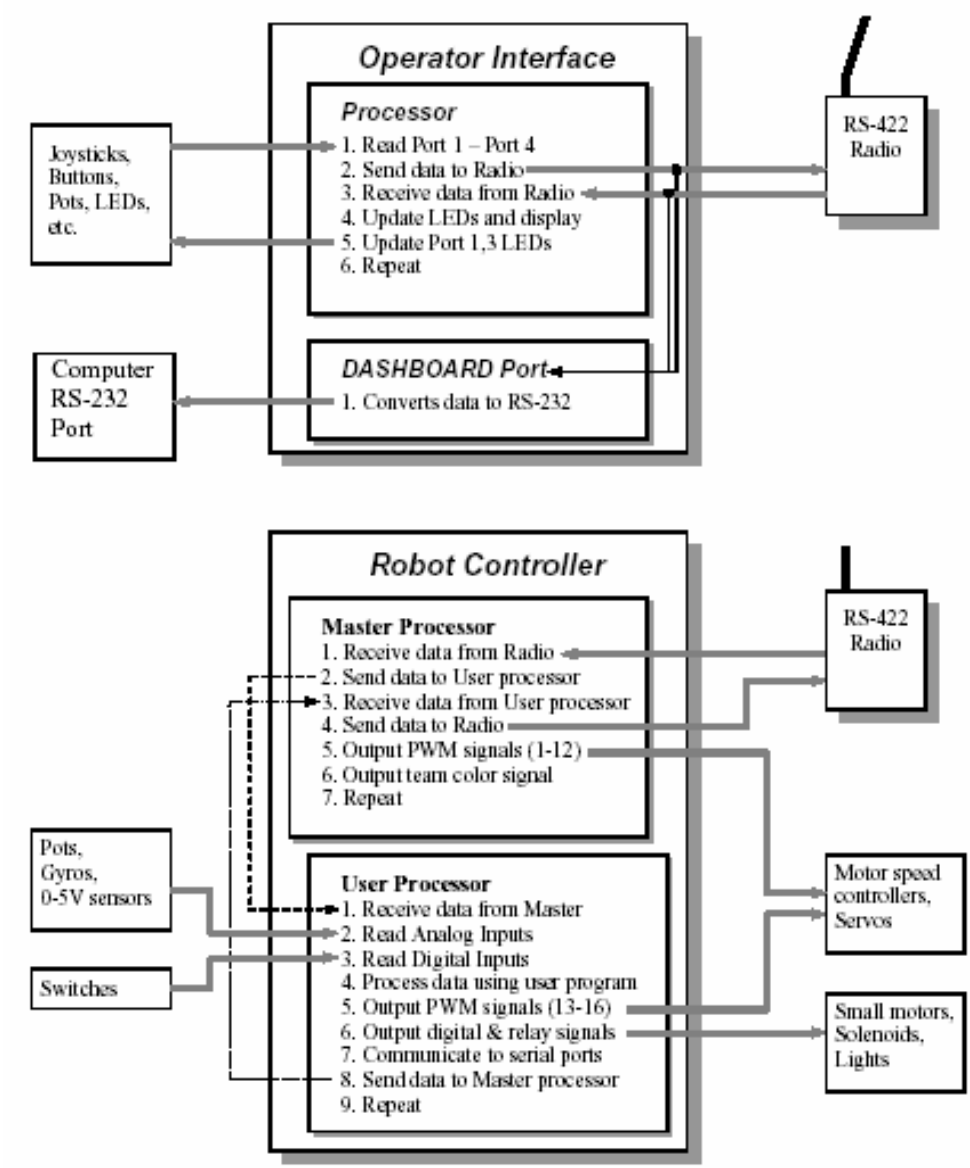

Courtesy of IFI Robotics. Used with permission.

Figure 2.4.3 Control system operation diagram, IFI, Inc.

2.5 Optical Shaft Encoders

The servomechanism described in the previous section is based on analogue feedback technology, using a potentiometer and a tachometer generator. These analogue feedbacks, although simple, are no longer used in industrial robots and other industrial applications, due to limited reliability and performance. A potentiometer, for example, is poor in reliability, resolution, accuracy, and signal to noise ratio. The output tap of the variable resistance slides on a track of resistive material, making a mechanical contact all the time. This slide contact causes not only electric noise but also wear of the contacting surfaces. The resolution and S/N ratio of the sensor are also limited by the mechanical contact. Furthermore, linearity depends on the uniformity of the resistive material coated on the substrate, and that is a limiting factor of a potentiometer's accuracy. Today's industrial standard is optical shaft encoders, having no sliding contact. This will be discussed next.

2.5.1 Basic principle

An optical encoder consists of a rotating disk with grids, light sources, photodetectors, and electronic circuits. As shown in Figure 2.5.1, a pattern of alternating opaque and translucent grids is printed on the rotating disk. A pair of light source and photodetector is placed on both sides of the rotating disk. As an opaque grid comes in, the light beam is blocked, while it is transmitted through the disk, when the translucent part comes in. The light beam is then detected by the photodetector. The disk is coupled to a motor shaft or a robot joint to measure. As it rotates, an alternating ON-OFF signal is obtained with the photodetector. The number of grids passing through the optical elements represents the distance traveled.

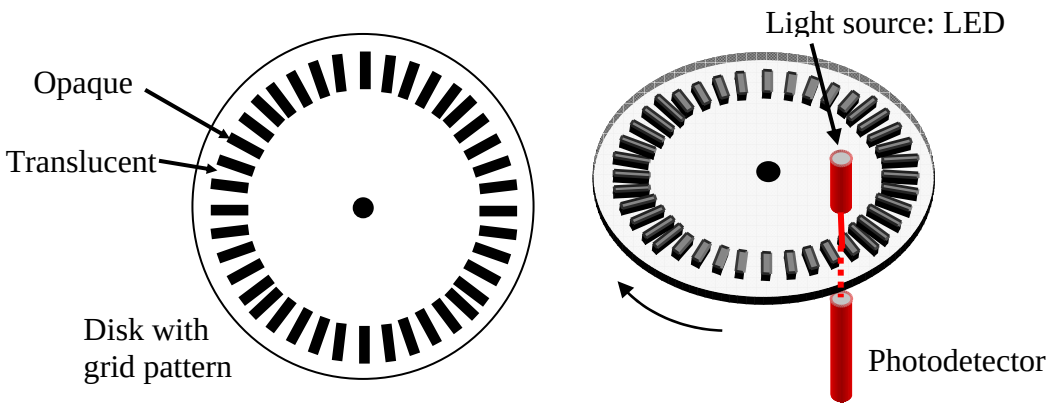

Figure 2.5.1 Basic construction of optical shaft encoder

This optical shaft encoder has no mechanical component making a slide contact, and has no component wear. An optical circuit is not disturbed by electric noise, and the photodetector output is a digital signal, which is more stable than an analogue signal. These make an optical shaft encoder reliable and robust; it is a suitable choice as a feedback sensor for servomotors.

2.5.2 Position measurement

One problem with the above optical encoder design is that the direction of rotation cannot be distinguished from the single photodetector output. The photodetector output is the same for both clockwise and counter-clockwise rotations. There is no indication as to which way the disk is rotating. Counting the pulse number merely gives the total distance the shaft has rotated back and forth. To measure the angular “position”, the direction of rotation must be distinguished.

One way of obtaining the directional information is to add another pair of light source/photodetector and a second track of opaque/translucent grids with 90 degrees of phase difference from the first track. Figure 2.5.2 illustrates a double track pattern and resultant output signals for clockwise and counter-clockwise rotations. Note that track A leads track B by 90 degrees for clockwise rotation and that track B leads track A for counter-clockwise rotation. By detecting the phase angle the direction of rotation can be distinguished, and this can be done easily with an up-down counter.

By simply feeding both A phase and B phase encoder signals to an up-down counter, the direction of rotation is first detected, and the number of rising edges and falling edges of both signals is counted in such a way that the counter adds the incoming edge number for clockwise rotation and subtract the edge numbers for counter-clockwise rotation. The up-down counter indicates the cumulative number of edges, that is, the angular “position” of the motor. The output of the up-down counter is binary *n*-bit signals ready to be sent to a digital controller without A/D conversion.

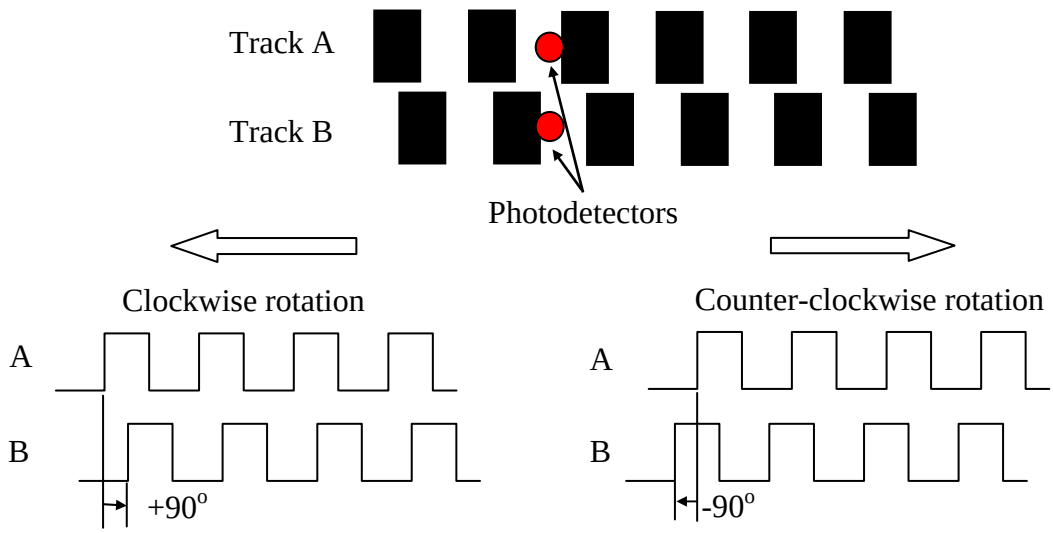

Figure 2.5.2 Double track encode for detection of the direction of rotation

It should be noted that this type of encoder requires initialization of the counter prior to actual measurement. Usually a robot is brought to a home position and the up-down counters are set to the initial state corresponding to the home position. This type of encoder is referred to as an ***incremental encoder***, since A-phase and B-phase signals provide relative displacements from an initial point. Whenever the power supply is shut down, the initialization must be performed for incremental encoders.

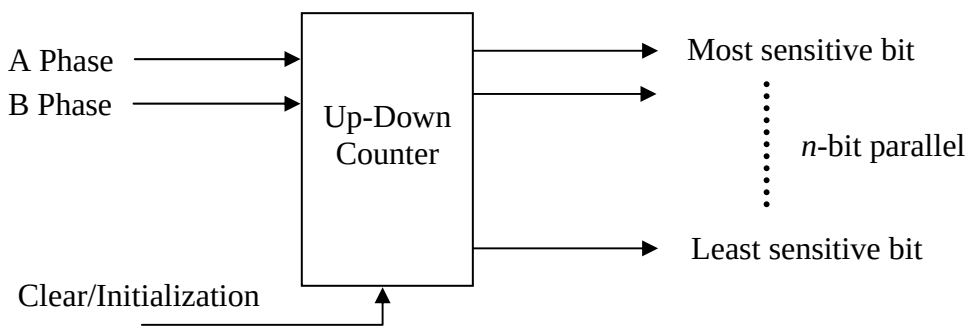

Figure 2.5.3 Up-down counter for an incremental encoder

An ***absolute encoder*** provides an *n*-bit absolute position as well as the direction of rotation without use of an up-down counter and initialization. As shown in Figure 2.5.4, the rotating disk has *n*-tracks of opaque-translucent grid patterns and *n* pairs of light sources and photodetectors. The *n*-tracks of grid patterns differ in the number of grids; the innermost track has only $1=2^0$ pair of opaque and translucent slits, the second track has $2=2^1$ pairs, and the *i*-th track has 2^{i-1} pairs. The *n* outputs from the photodetectors directly indicate the *n*-bit absolute position of the rotating disk. In general, absolute encoders are more complex and expensive than incremental encoders. In case of power failure, incremental encoders need a laborious

initialization procedure for recovery. For quick recovery as well as for safety, absolute encoders are often needed in industrial applications.

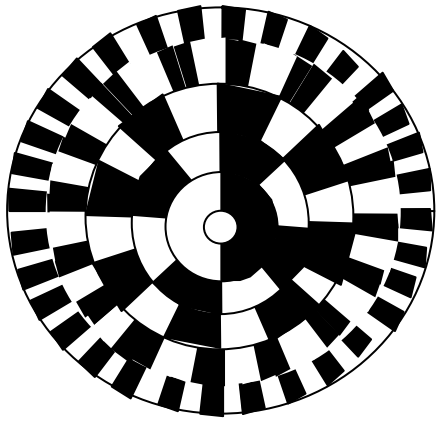

Sorry for this poor drawing. I did in haste.

Figure 2.5.4 Absolute encoder

2.5.3 Velocity estimate

Velocity feedback is needed for improving accuracy of speed control as well as for compensating for system dynamics. A salient feature of optical encoders is that velocity information can be obtained along with position measurement. Without use of a dedicated tachometer generator, velocity measurement can be attained by simply processing pulse sequences generated by an optical encoder.

Figure 2.5.5 shows a pulse sequence coming from an optical encoder.[2] Each pulse indicates a rising edge or a falling edge of phase A & B signals. Therefore, the density of this pulse train, i.e. the pulse frequency, is approximately proportional to the angular velocity of the rotating shaft. The pulse density can be measured by counting the number of incoming pulses in every fixed period, say T=10 *ms*, as shown in the figure. This can be done with another up-down counter that counts A phase and B phase pulses. Counting continues only for the fixed sampling period T, and the result is sent to a controller at the end of every sampling period. Then the counter is cleared to re-start counting for the next period.

As the sampling period gets shorter, the velocity measurement is updated more frequently, and the delay of velocity feedback gets shorter. However, if the sampling period is too short, discretization error becomes prominent. The problem is more critical when the angular velocity is very small. Not many pulses are generated, and just a few pulses can be counted for a very short period. As the sampling period gets longer, the discretization error becomes smaller, but the time delay may cause instability of the control system.

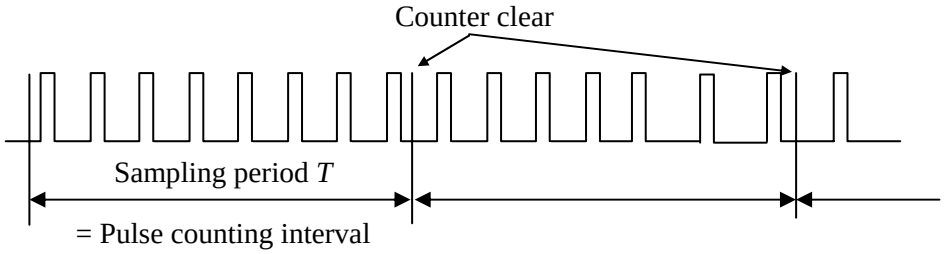

Figure 2.5.5 Velocity estimate based on pulse frequency measurement

[2] For simplicity only an incremental encoder is considered.

An effective method for resolving these conflicting requirements is to use a dual mode velocity measurement. Instead of counting the number of pulses, the *interval* of adjacent pulses is measured at low speed. The reciprocal to the pulse interval gives the angular velocity. As shown in Figure 2.5.6, the time interval can be measured by counting clock pulses. The resolution of this pulse interval measurement is much higher than that of encoder pulse counting in a lower speed range. In contrast, the resolution gets worse at high speed, since the adjacent pulse interval becomes small. Therefore, these two methods supplement to each other. The dual mode velocity measurement uses both counters and switches them depending on the speed.

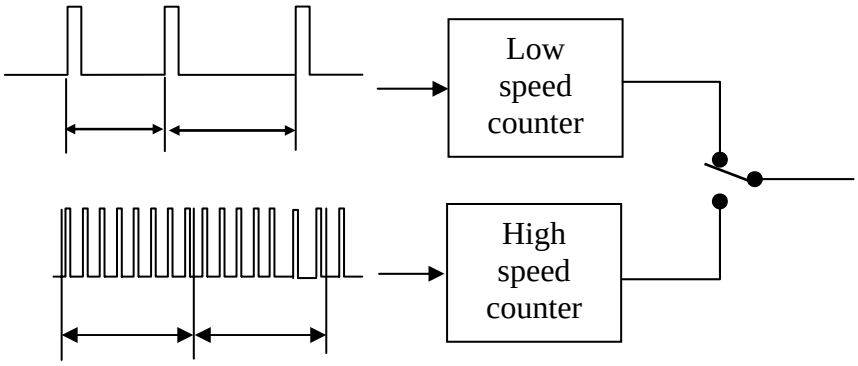

Figure 2.5.6 Dual mode velocity measurement

2.6 Brushless DC Motors

The DC motor described in the previous section is the simplest, yet efficient motor among various actuators applied to robotic systems. Traditional DC motors, however, are limited in reliability and robustness due to wear of the brush and commutation mechanism. In industrial applications where a high level of reliability and robustness is required, DC motors have been replaced by brushless motors and other types of motors having no mechanical commutator. Since brushless motors, or AC synchronous motors, are increasingly used in robotic systems and other automation systems, this section briefly describes its principle and drive methods.

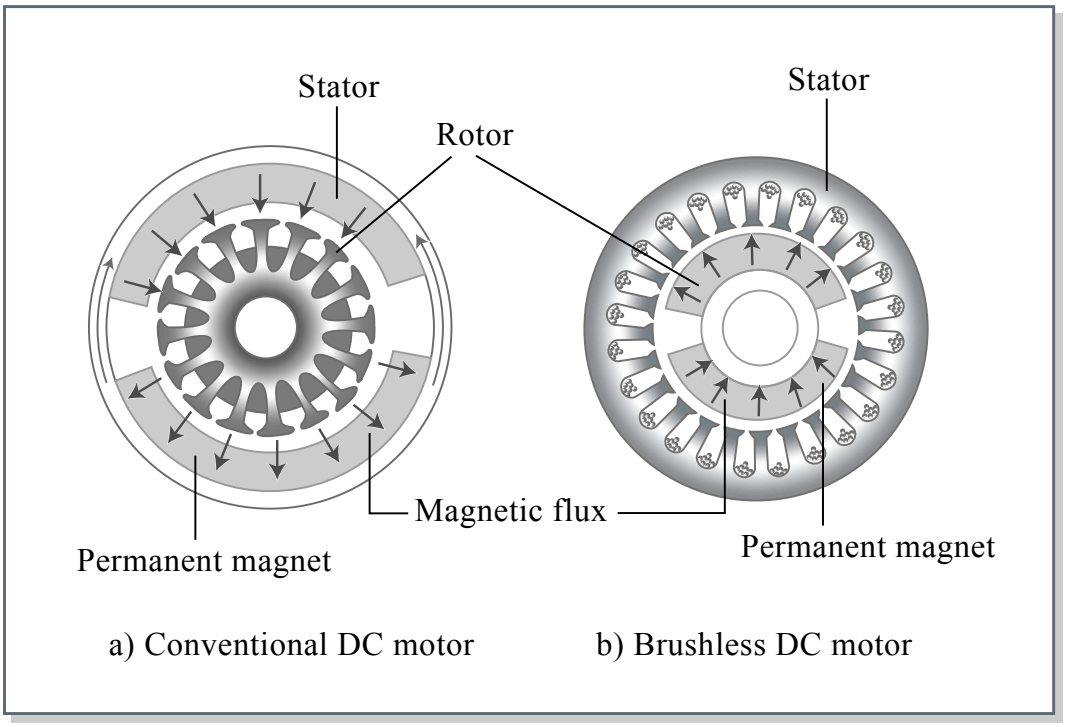

Figure by MIT OCW.

Figure 2.6.1 Construction of brushless DC motor and conventional DC motor

In the brushless motor, the commutation of currents is performed with an electronic switching system. Figure 2.6.1 shows the construction of a brushless motor, compared with a traditional DC motor. In the brushless motor, the rotor and the stator are swapped. Unlike the traditional DC motor, the stator of the brushless motor consists of windings, whereas the rotor comprises permanent magnets. The commutation is accomplished by measuring the rotor position using a position sensor. Depending on the rotor position, currents are delivered to the corresponding windings though electronic switching circuits. The principle of torque generation remains the same, and the torque-speed characteristics and other properties are mostly preserved. Therefore, the brushless motor is highly efficient with added reliability.

A drawback of this brushless motor design is that the torque may change discontinuously when switches are turned on and off as the rotor position changes. In the traditional DC motor this torque ripple is reduced by simply increasing the commutator segments and dividing the windings to many segments. For the brushless motor, however, it is expensive to increase the number of electronic switching circuits. Instead, in the brushless motor the currents flowing into individual windings are varied continuously so that the torque ripple be minimum. A common construction of the windings is that of a three-phase windings, as shown in Figure 2.6.2.

Let I_A, I_B and I_C be individual currents flowing into the three windings shown in the figure. These three currents are varies such that:

$$\begin{aligned} I_A &= I_O \sin\theta \\ I_B &= I_O \sin(\theta + \frac{2}{3}\pi) \\ I_C &= I_O \sin(\theta + \frac{4}{3}\pi) \end{aligned} \tag{2.6.1}$$

where I_O is the scalar magnitude of desired current, and θ is the rotor position. The torque generated is the summation of the three torques generated at the three windings. Taking into account the angle between the magnetic field and the force generated at each air gap, we obtain

$$\tau_m = k_O[I_A \sin\theta + I_B \sin(\theta + \frac{2}{3}\pi) + I_C \sin(\theta + \frac{4}{3}\pi)] \tag{2.6.2}$$

where k_0 is a proportionality constant. Substituting eq.(1) into eq.(2) yields

$$\tau_m = \frac{2}{3} k_O I_O \tag{2.6.3}$$

The above expression indicates a linear relationship between the output torque and the scalar magnitude of the three currents. The torque-current characteristics of a brushless motor are apparently the same as the traditional DC motor.

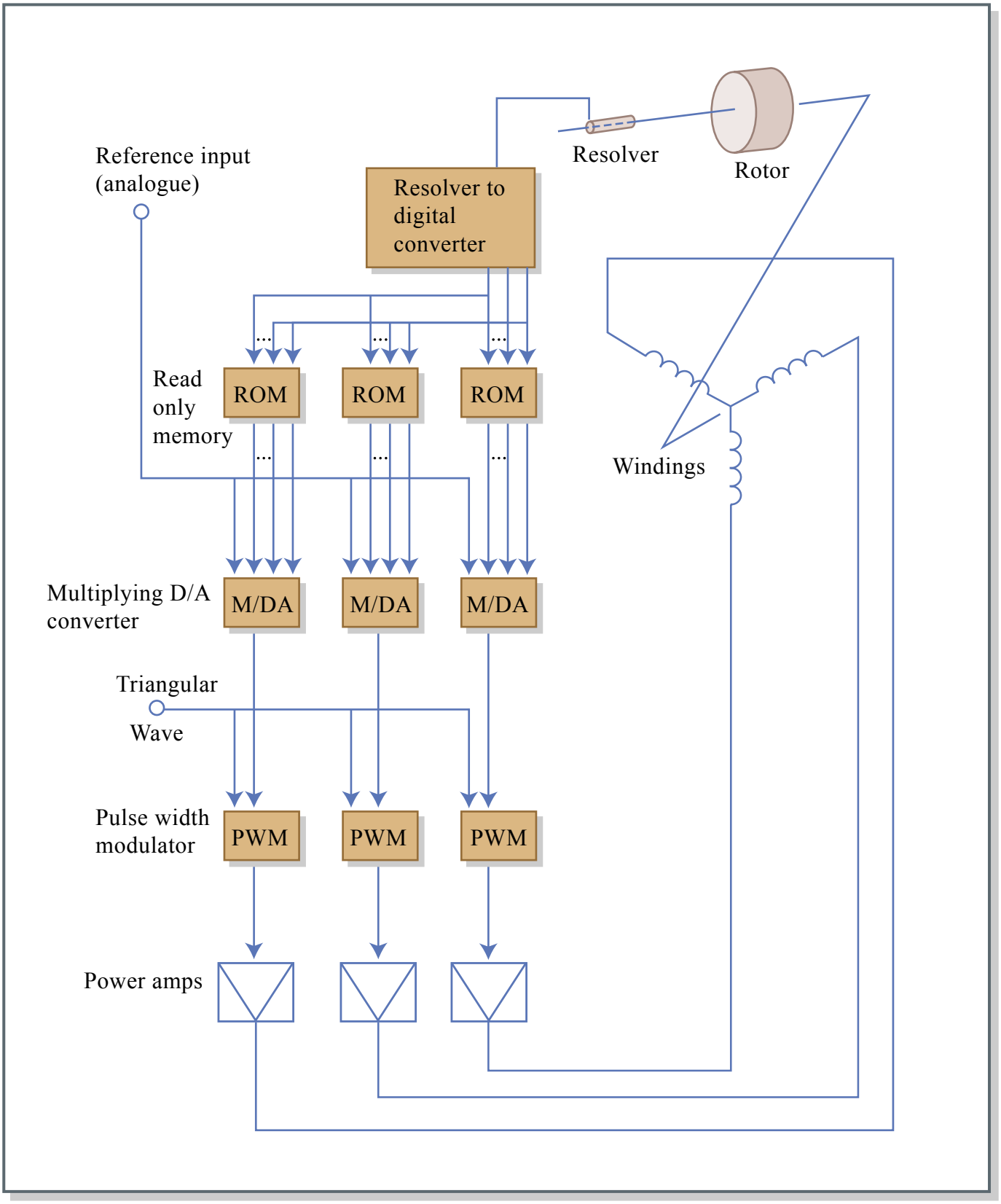

Figure 2.6.2 Brushless DC motor and drive amplifier

Figure by MIT OCW.